Journal of Arid Environments 117 (2015) 67–74

Contents lists available at ScienceDirect

Journal of Arid Environments

journal homepage: www.elsevier.com/locate/jaridenv

Effects of soil water content, temperature and experimental nitrogen deposition on nitric oxide (NO) efflux from semiarid shrubland soil

George L. Vourlitis*, Catherine DeFotis, William Kristan

Department of Biological Sciences, California State University, San Marcos 92096, USA

ARTICLE INFO

Article history:
Received 8 September 2014
Received in revised form
3 February 2015
Accepted 10 February 2015
Available online

Keywords:
Anthropogenic nitrogen deposition
Arrhenius equation
Chaparral
Global change
Nitrogen cycle
Semi-arid ecosystems

ABSTRACT

Southern Californian urban shrublands are exposed to high nitrogen (N) deposition, which can potentially enhance soil nitric oxide (NO) efflux; however, environmental controls on NO emission are still uncertain. We conducted a laboratory experiment to evaluate the NO efflux response of chaparral soil to variations in N availability, temperature and moisture. We hypothesized that NO efflux would increase with N addition, have an optimum response to soil moisture, and increase exponentially with temperature. Our results supported our hypotheses. Nitrogen addition caused a linear increase in NO efflux, primarily because of an increase in NH_4^+. NO efflux reached a peak at intermediate soil moisture (25% water-filled pore space (WFPS)), and the temperature response of NO flux was well-described by the Arrhenius model. However, there were statistically significant interactions between N, temperature and soil water content, making the NO response complex. Our results suggest that southern California urban shrublands may be important sources of NO, and that chronic, high levels of anthropogenic N deposition will enhance NO efflux from these ecosystems.

1. Introduction

Human alteration of the nitrogen (N) cycle is a significant global-scale problem (Vitousek et al., 1997; Townsend et al., 2003; Galloway et al., 2004; Fenn et al., 2008), and chronic, high levels of anthropogenic N inputs can lead to "N saturation," where N inputs exceed ecosystem N storage capacity (Aber et al., 1989; Fenn et al., 2003b, 2008; Vourlitis and Fernandez, 2012; Homyak et al., 2014). This is especially true for urban areas of southern California, which are "hot spots" for air pollution and atmospheric N deposition (Bytnerowicz and Fenn, 1996; Fenn et al., 2003a). Urban shrublands of the Los Angeles, Riverside, and San Bernardino basins receive an estimated 25–45 kgN ha^{-1} a^{-1} (Fenn et al., 2003a; Meixner and Fenn, 2004); however, exposed high elevation chaparral and coniferous forests may receive up to 145 kgN ha^{-1} a^{-1} from throughfall of inorganic N that accumulates on tree and shrub biomass (Fenn and Poth, 2004).

High rates of anthropogenic N deposition have the potential to amplify gaseous N losses (Davidson, 1992; Vitousek et al., 1997; Skiba et al., 2004; Homyak and Sickman, 2014; Homyak et al., 2014); thus, one of our main goals was to evaluate how gaseous N emission varied as a function of experimental N input. According to the "hole-in-pipe" model (Firestone and Davidson, 1989), an increase in N deposition can enhance nitric oxide (NO) and/or nitrous oxide (N_2O) emissions because of an increase in nitrification, the microbial oxidation of NH_4^+ to nitrate (NO_3^-), and/or denitrification, the microbial reduction of NO_3^- to nitrite (NO_2^-), NO, nitrous oxide (N_2O), and ultimately N_2. However, the relative proportions of NO and N_2O also depend on other factors such as soil moisture and temperature (Davidson, 1991; Remde and Conrad, 1991; Roelle et al., 2002; Schindlbacher et al., 2004). For example, low soil moisture can limit rates of denitrification more than nitrification, thus favoring NO efflux relative to N_2O, while high soil moisture can limit rates of nitrification more than denitrification, thus favoring N_2O efflux over NO (Davidson, 1991). For this reason, NO efflux tends to be higher in low-intermediate soil moistures depending on soil type (Andersen and Poth, 1989; Schindlbacher et al., 2004); however, re-wetting of soil after long periods of drought can lead to large transient losses of NO from semi-arid soils (Homyak and Sickman, 2014). N_2O and NO emissions also increase with soil temperature, provided that other factors, such as soil moisture, are not limiting, because of a concomitant increase in enzyme kinetics (Roelle et al., 2002; Schindlbacher et al., 2004).

Interactions between N availability and other environmental

* Corresponding author.
E-mail address: georgev@csusm.edu (G.L. Vourlitis).

http://dx.doi.org/10.1016/j.jaridenv.2015.02.011
0140-1963/

factors, such as soil temperature and moisture, on NO emissions are still poorly understood, especially in urban semi-arid chaparral shrublands where episodically high N losses are thought to be a symptom of N saturation (Fenn et al., 2008; Vourlitis and Fernandez, 2012; Homyak et al., 2014). However, chaparral exhibits high rates of nitrification (Sirulnik et al., 2007; Vourlitis et al., 2007a, b, 2009; Vourlitis and Zorba, 2007; Vourlitis and Fernandez, 2012), regardless of N input, and pulsed resource dynamics that can result in high rates of N losses followed by periods of N storage (Meixner and Fenn, 2004; Vourlitis et al., 2007a; Vourlitis and Fernandez, 2012; Homyak et al., 2014). Thus, to better understand how N enrichment interacts with soil environmental factors to affect NO efflux from semi-arid shrubland soils we conducted a short-term laboratory incubation experiment that simultaneously manipulated soil N availability, temperature, and water content. We focused on NO efflux because previous research in semi-arid chaparral soils suggests that NO emissions are approximately 3-orders of magnitude higher than N_2O emissions (Andersen and Poth, 1989; Fenn et al., 1996). Based on previous research, we hypothesized that NO efflux from southern California chaparral soils would i) increase as a function of N addition, ii) have an optimum response to variations in soil moisture, and iii) increase as a function of temperature.

2. Materials and methods

2.1. Field sampling and laboratory analysis

Surface soil from the upper 10 cm layer (A-horizon) was collected in September 2008 from a chaparral stand located on a flat hilltop at California State University, San Marcos in San Diego County, California, USA. The vegetation of the field site was a Chamise-Black Sage series chaparral (Sawyer and Keeler-Wolf, 1995), which was dominated by *Adenostoma fasciculatum* Hook & Arn. (Chamise), *Salvia mellifera* Green (Black sage), and *Eriogonum fasciculatum* Benth. (California buckwheat). The soil type is a coarse sandy-loam of the Cieneba series, which are Typic Xerorthents (Bowman et al., 1973). Average bulk density is 1.34 g/cm^3, and average (±1sd) total soil N and C are 0.22 ± 0.01% and 3.27 ± 0.16%, respectively. Average (±1sd) extractable NH_4^+ is 9.7 ± 0.8 μg N/g dry soil (1.30 g N/m^2) and average extractable NO_3^- is 12.3 ± 1.8 μg N/g dry soil (1.65 g N/m^2).

Soil samples were collected using a 4.7 cm diameter × 10 cm deep (173.5 cm^3) bucket auger from approximately 20 random locations. Samples were immediately returned to the lab to be air-dried and stored at room temperature until laboratory incubations and analyses were completed. In the lab, the soil was sieved (Test Sieve No. 10, mesh size = 2 mm, Newark Wire Cloth Company, Clifton, NJ, USA) and homogenized to eliminate organic and mineral material >2 mm, and all samples were mixed to achieve a uniform composite soil (Cho and Peirce, 2005). The initial soil water content was determined by weighing fresh soil samples (Sartorius MC1 Analytic AC 210S, Data Weighing Systems, Elk Grove, IL), oven-drying (Gravity Oven GO1350C-1, Lindberg/Blue, Asheville, NC, USA) at 105 °C for 4 days, and reweighing them to account for the loss in soil moisture.

2.2. N addition experiment

To determine the relationship between N addition and NO flux, 25 g of air-dried soil was weighed into 56 cm^3 (5.7 cm^2 diameter × 9.9 cm tall) sterile polystyrene incubation chambers (BD Falcon, Franklin Lakes, NJ, USA) and exposed to 0, 2, 4, and 6 g N/m^2 (n = 6 per treatment) in the form of granular ammonium sulfate ($(NH_4)_2SO_4$), which encompasses the typical N deposition gradient in southern California (Fenn et al., 2003a). Given a soil background level of approximately 3.0 g N/m^2 for extractable NH_4^+ and NO_3^- combined (see section 2.1 above), total extractable N inputs for the N treatments above were approximately 3, 5, 7, and 9 g N/m^2 (0.07, 0.11, 0.16, and 0.20 mg N/g dry soil, respectively). We used $(NH_4)_2SO_4$ because rates of nitrification are high in these soils (Sirulnik et al., 2007; Vourlitis et al., 2007a, b; 2009; Vourlitis and Zorba, 2007; Vourlitis and Fernandez, 2012) and we were interested in relating the NO efflux to the rate of nitrification. Thus, we did not want to add a NO_3 source to the experimental soil. Soil moisture levels were brought to 15% (by weight) by adding deionized water, which following Linn and Doran (1984) corresponded to 42% water-filled pore space (WFPS = (θ_v/TP)*100; where θ_v is the percent volumetric soil water content calculated as the product of percent gravimetric water content and bulk density and TP is the total soil porosity = 1 − (bulk density/particle density) × 100, assuming that the particle density is 2.65 g/cm^3). After wetting, soil was shaken until it appeared to be uniformly mixed and wet. Following Varella et al. (2004), the incubation chambers were covered with Parafilm to allow gas exchange but reduce water loss and left at room temperature for 24 h before NO flux measurement.

Soil NH_4^+ and NO_3^- was extracted after NO flux measurements to measure inorganic N availability. Ten grams of soil from each sample was weighed into 125 ml Erlenmeyer flasks and exposed to 40 ml of 0.5 M K_2SO_4. The flasks were placed on an orbital shaker table (Max Q 2000, Barnstead International, Dubuque, IA) for 1 h and the supernatant was filtered into plastic sample bottles (1 oz. wide mouth, Fischer Scientific, Santa Clara, CA) using glass funnels and filter paper (0.2 μm; No.1–125 mm, Whatman International Ltd., Maidstone, England). Extracts were stored at −20 °C until analysis, and NH_4^+ and NO_3^- concentrations were analyzed with a flow injection analyzer (Lachet Quikchem 3000, Lachet Instruments, Milwaukee, WI, USA) using QuikChem Methods 12-107-04-1B and 12-107-06-2-A, respectively.

2.3. Soil nitrogen, moisture and temperature experiment

A second experiment was conducted to determine the interactions between soil N availability, moisture, and temperature on NO flux. As in the previous experiment, 25 g of air-dried field soil was weighed into 56 cm^3 sterile polystyrene incubation chambers. Soil moisture levels were brought to 3.7, 8.9, 20.3, and 25.7% water (by weight) by adding deionized water, which corresponded to 10.5, 25.0, 57.3, and 72.7% WFPS (n = 5 per treatment). These soil moistures were used because they span a wide range of potential soil moisture for southern Californian chaparral soils, with 8.9 and 3.7% water (by weight) being the average soil moisture observed during the spring and summer, respectively (Vourlitis et al., 2007a). Nitrogen was added in the form of granular $(NH_4)_2SO_4$, at levels of 0 (control), 2, and 5 g N/m^2, which given the background level of 3.0 g N/m^2, corresponded to an available N of approximately 3 (control), 5, and 8 g N/m^2, or 0.07, 0.11, and 0.18 mg N/g dry soil, respectively. After the N and water were added, the soil within the incubation chamber was shaken to ensure uniform wetting and fertilization. Incubation chambers were left at room temperature for 24 h and covered with Parafilm to reduce water loss.

After a 24 h incubation period, NO fluxes were measured as described below (section 2.4). Soil temperatures were measured prior to each NO flux measurement by inserting a thermocouple probe into the first 3 cm of soil within each tube. The NO flux was first measured at room temperature (ca. 25 °C), then all incubation chambers were transferred to an ice-water bath (ca. 2 °C), and then a hot-water bath (ca. 35 °C; Chicago Surgical and Electrical Company, Chicago, IL) to measure the NO efflux under varying

temperatures. Soil temperature adjusted rapidly (typically within 1–5 min) after incubation chambers were moved to a new temperature, and NO efflux was measured after soil temperature stabilized to the new temperature treatment. This temperature range was used because it is a typical maximum and minimum annual soil temperature range for chaparral soils (Johnson-Maynard et al., 2004). After NO flux was measured, soil NH_4^+ and NO_3^- were extracted as described above.

2.4. NO flux measurements

NO was measured using a chemiluminescence analyzer (Model 42i, Thermo Electron Corporation, Waltham, MA, USA). The analyzer was an open system that vented to the atmosphere at a constant flow rate of 0.3 L/min. However, at this flow rate, the chamber volume (50 ml) exchanged rapidly (i.e., every 10 s), which was too rapid for the NO efflux to equilibrate to the airflow and allow fluxes to be measured in a true open-system mode. Thus, we used the NO analyzer like a gas chromatograph and injected the NO that accumulated within each incubation chamber over 1, 5, and 10-min intervals. For each measurement, the incubation chamber was affixed with a screw-top cap that was perforated with two pieces of 4.4 mm diameter (inside) Teflon tubing, one piece was approximately 10 cm long and reached to the soil incubating inside the chamber (the chamber outflow) and the other was approximately 4 cm long and allowed ambient air to enter and equalize the pressure between the incubation chamber and the ambient air during measurement. During each measurement, the chamber outflow tube was attached to the NO analyzer inlet, and the entire volume of air in the chamber headspace was evacuated. As the chamber atmosphere was analyzed by the chemiluminescence detector, the NO density ($\mu gN\ m^{-3}$) increased, reached a maximum value, and then declined back to the ambient baseline, a process that took approximately 15–30 s. With a sensor response time of 1 s, the maximum NO density based on factory software and calibration was recorded for each measurement. The maximum density was taken as the chamber NO density, because with chamber mixing by the pump, the maximum density is likely the closest to the average NO density that accumulated within the chamber headspace during incubation.

After each measurement, the incubation chamber was detached from the NO analyzer, the Teflon tubing was clamped to eliminate gas exchange between the chamber and ambient atmosphere, the incubation chamber was returned to the appropriate incubation environment, and NO was allowed to accumulate for the appropriate (i.e., 1, 5, or 10 min) amount of time. NO flux was calculated from linear regression as the change in maximum NO density (dependent variable) as a function of incubation time (independent variable) over the measurement period. Average (±SD) coefficients of determination (r^2) values were approximately 0.95 ± 0.05, indicating a linear change in NO density during the measurement period.

2.5. Statistical analyses

All data were analyzed using Number Cruncher Statistical System software (NCSS V7.1.12; Hintz, 2004). Linear regression was used to determine the functional relationship between N addition, extractable NH_4^+, extractable NO_3^- (independent variables), and NO (dependent variable). The Arrhenius equation was used to determine the temperature response of NO flux due to its ability to model the relationship between temperature and biologically mediated processes across the temperature range 0–40 °C (Fang and Moncrieff, 2001; Sjögersten and Wookey, 2002; Schindlbacher et al., 2004). NO efflux data were log transformed before analysis to linearize the response (Schindlbacher et al., 2004). The activation energy (E_a; kJ/mol), which is an estimate of microbial temperature sensitivity, was calculated by the Arrhenius equation (equ. 1),

$$\mathrm{LN}(F_{NO}) = \mathrm{LN}(\alpha) - E_a/RT \quad (1)$$

where α is the frequency factor, R is the universal gas constant (8.314 J K^{-1} mol^{-1}), and T is the soil temperature (K). E_a was determined from the slope of the linear regression line of the inverse temperature (independent variable) versus ln NO flux (dependent variable). A three-way analysis of variance (ANOVA) was used to test the effects of added N, soil moisture, and soil temperature on NO efflux. Two-way ANOVA was used to test the effects of soil moisture and N addition on the Arrhenius intercept and E_a.

3. Results

3.1. Effects of N addition on soil N availability and NO efflux

Mean (±standard error (SE), n = 6) soil extractable NH_4^+ concentration increased linearly with experimental N addition (Fig. 1a), but NO_3^- concentration remained unchanged (Fig. 1b). The increase in N availability led directly to an increase in NO efflux (Fig. 2a). Mean (±SE, n = 6) NO flux increased linearly with added N (Fig. 2a), and this increase was due almost entirely to an increase in NH_4^+ availability (Fig. 2b), as the correlation between extractable NO_3^-

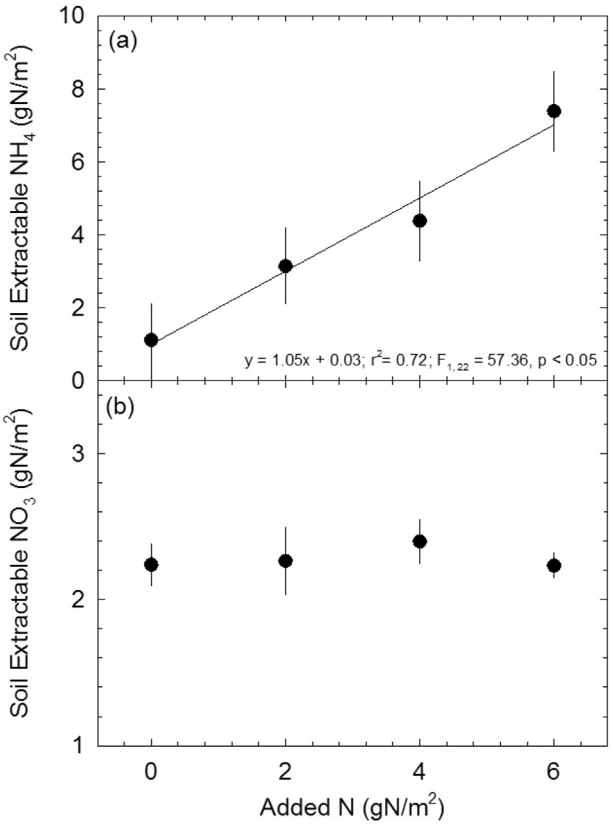

Fig. 1. The mean (±SE, n = 6) soil extractable NH_4^+ (a) and NO_3^- (b) as a function of added N. Shown is the best-fit line and equation calculated using linear regression, coefficient of determination (r^2), and the p-value. Note that with panels lacking a regression line the linear trend was not significantly different from zero. Measurements were taken from samples at room temperature and 42% water-filled pore space (WFPS).

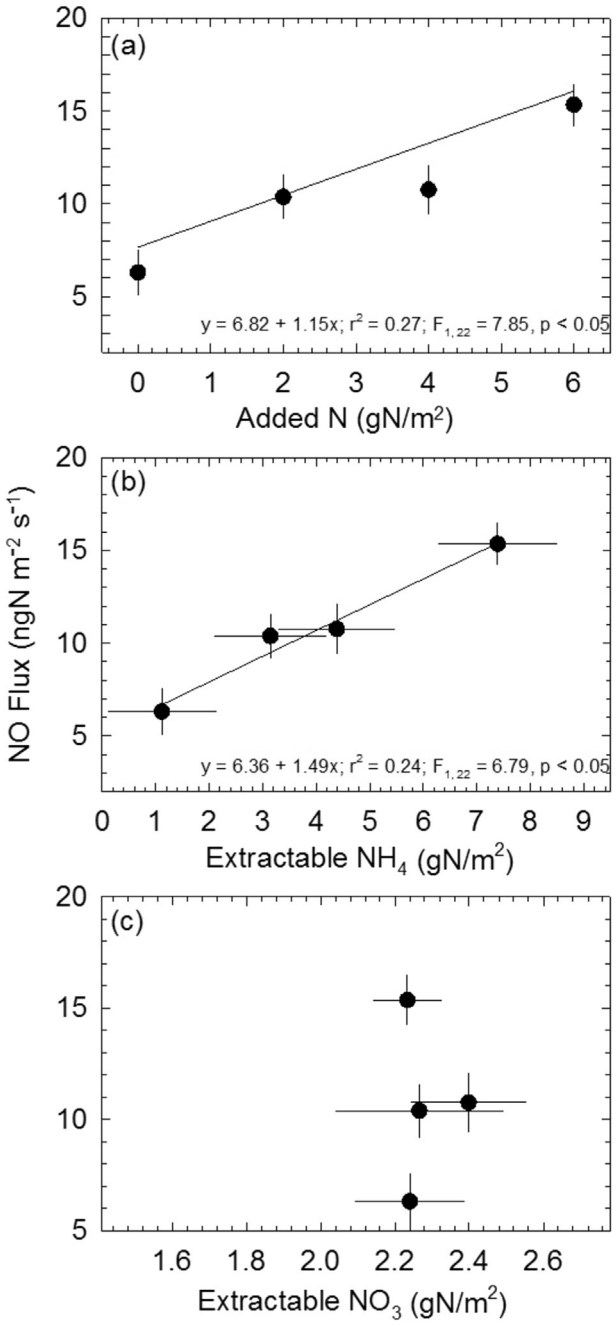

Fig. 2. The mean (±SE, n = 6) NO flux as a function of added N (a), soil extractable NH_4^+ (b), and NO_3^- (c). Also shown is the best-fit line and equation calculated using linear regression and the coefficient of determination (r^2). Note that with panels lacking a regression line the linear trend was not significantly different from zero. Measurements were taken from samples at room temperature and 42% water-filled pore space (WFPS).

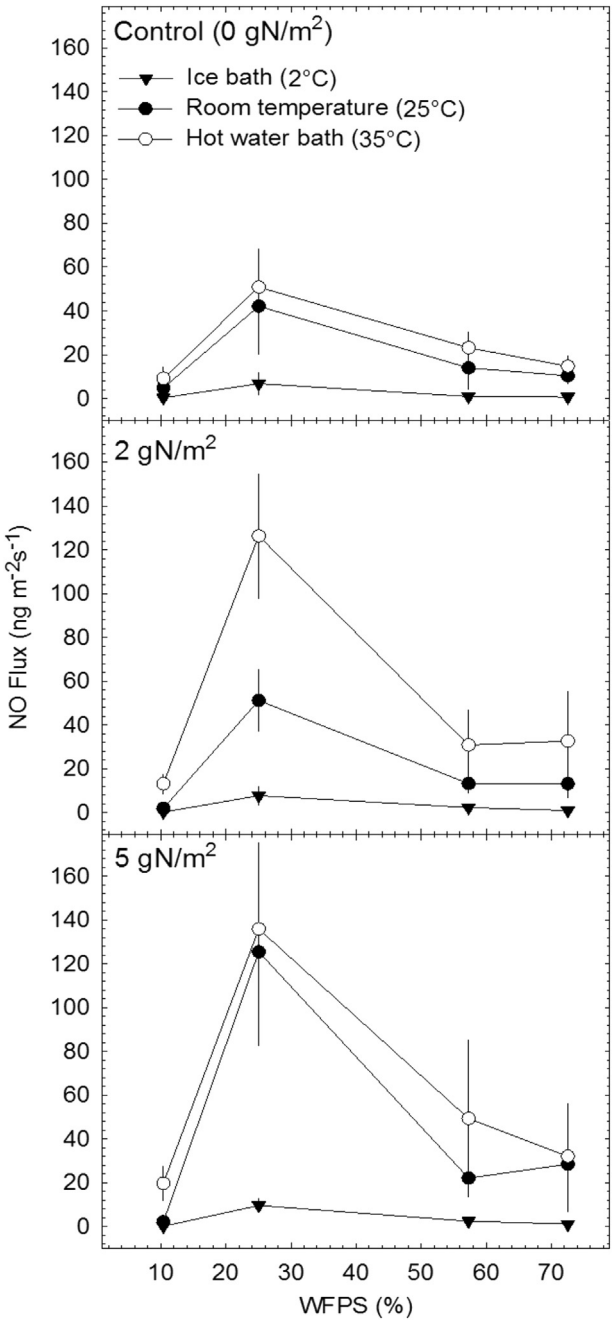

Fig. 3. The mean (±SE, n = 5) NO flux as a function of water-filled pore space (WFPS) and temperature in soil exposed to 0 g N/m^2 (control; top panel), 2 g N/m^2 (middle-panel), and 5 g N/m^2 (top-panel). The plotting symbols indicate temperature treatments; ice-water bath (inverted-triangles), room temperature (black-circles), and hot-water bath (white-circles).

and NO was not statistically significant ($p > 0.05$; Fig. 2c).

3.2. Interactions between NO flux, N addition, soil moisture, and temperature

Mean (±SE, n = 5) instantaneous NO fluxes (ngN m^{-2} s^{-1}) increased significantly as a function of added N and temperature, but with soil moisture there was a consistent optimum at approximately 25% water-filled pore space (WFPS) (Fig. 3). In general, NO efflux was highest in the 5 g N/m^2, hot-water bath (ca. 35 °C), and 25% WFPS treatment combination, however, the NO flux response to the treatments was complex leading to significant 2- and 3-way interactions (Table 1; Fig. 3). NO flux from soil exposed to the ice bath temperature treatment (ca. 2 °C) was substantially lower than the other temperature treatments at 25% WFPS and above, and NO flux varied from a peak of 6.7–9.7 ngN m^{-2} s^{-1} in the 25% WFPS treatment to a low of 0.17–0.33 ngN m^{-2} s^{-1} in the 10.5% WFPS treatment. Differences in NO flux from soil exposed to the room temperature (ca. 25 °C) and 35 °C varied as a function of added N and soil water content. In the low N (control) treatment,

Table 1
Three-way analysis of variance results displaying the effects of added N (N), soil moisture (W), and soil temperature (T°) on NO efflux.

Source of variation	DF	Sum of squares	Mean square	F-ratio	p value
Nitrogen (N)	2	13,162	6581	16.3	<0.001
Soil moisture (W)	3	84,596	28,199	69.9	<0.001
Temperature (T)	2	53,075	26,538	65.8	<0.001
N × W	6	13,639	2273	5.6	<0.001
N × T	4	9231	2308	5.7	<0.001
W × T	6	33,430	5572	13.8	<0.001
N × W × T	12	11,314	943	2.3	<0.01
Error	144	58,118	404		
Total	180	276,566			

NO flux in the 25 °C and 35 °C treatments increased from the 10.5% WFPS, reached a peak of 42.2 and 50.9 ngN m^{-2} s^{-1}, respectively at 25% WFPS, and declined as WFPS increased (Fig. 3). In the intermediate N (2 g N/m^2) treatment, NO flux at 35 °C/25% WFPS was >2-times higher than in the 25 °C/25% WFPS temperature treatment (Fig. 3), while in the highest N treatment (5 g N/m^2), differences in NO flux between the 25 and 35 °C treatments at 25% WFPS became negligible (Fig. 3).

The temperature response of NO flux was well-described by the Arrhenius model, with coefficient of determination (r^2) values ranging from 0.66 to 0.93 (Fig. 4; Table 2). However, there was a significant interaction between soil water content (WFPS) and soil temperature such that the intercept and the activation energy (E_a) of the Arrhenius model depended on WFPS (Table 2). Values of E_a ranged from 42.4 to 113.6 kJ mol^{-1}, with the lowest values observed in the 25% WFPS treatment and the highest values observed in 10.5% WFPS treatment (Table 2). Variations in the intercept were more complex, with the highest values observed in the 10.5% and 72.7% WFPS treatments (Table 2).

4. Discussion

4.1. Effects of N addition on extractable N and NO flux

Our results support the hypothesis that NO efflux from chaparral soil would increase with experimental N addition, which has implications for N cycling in urban shrublands exposed to chronic, high rates of atmospheric N deposition (Fenn et al., 2003b; Vourlitis and Fernandez, 2012; Homyak and Sickman, 2014). According to the conceptual "hole-in-pipe" model of gaseous N production (Firestone and Davidson, 1989), NO flux is regulated in part by the amount of N cycling through the ecosystem (the size of the pipe). NO efflux was significantly correlated with soil extractable NH_4^+, but not NO_3^-, which is somewhat surprising given that NO emission is a byproduct of nitrification and/or denitrification (Firestone and Davidson, 1989; Davidson, 1991). Furthermore, extractable NO_3^- was not correlated with N ($(NH_4)_2SO_4$) addition (Fig. 1b), which is in contrast to previous research that indicated that experimental N addition increased nitrification rates in semi-arid soils (Fenn et al., 1996; Vourlitis and Zorba, 2007; Vourlitis et al., 2007a, b; Sirulnik et al., 2007). However, it is possible that the short incubation period (24 h) was not long enough to result in a significant increase

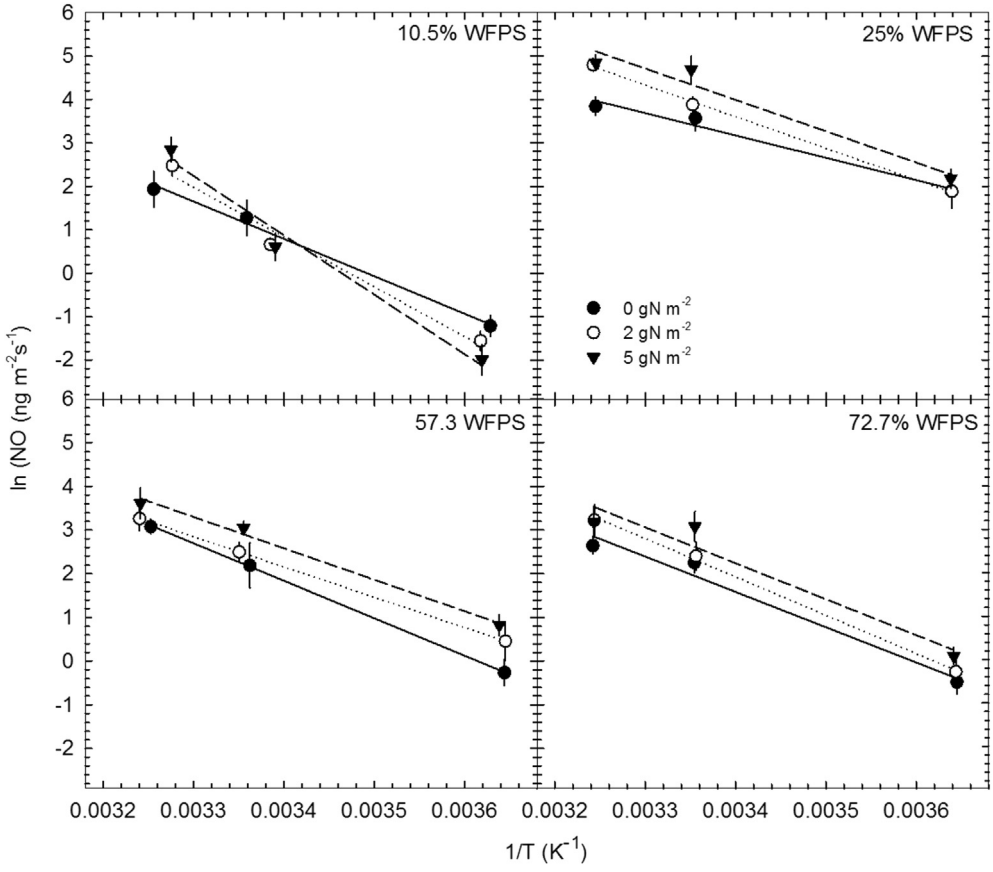

Fig. 4. Arrhenius plots with ln NO flux (±SE, n = 5) as a function of inverse temperature (K^{-1}) at 10.5% (top-left panel); 25% (top-right panel); 57.3% (bottom-left panel); and 72.7% (bottom-right panel) water-filled pore space (WFPS). The plotting symbols indicate ammonium sulfate ($(NH_4)_2SO_4$) addition levels; 0 g N/m^2 (solid-lines and closed-circles), 2 g N/m^2 (dotted-lines and open-circles), and 5 g N/m^2 (dashed-lines and inverted-triangles). Note that the corresponding line patterns represent regression lines (see Table 2 for regression statistics).

Table 2
Mean (±95% confidence interval; n = 5) y-intercept (b) and activation energy (E_a) calculated from Arrhenius plots of the ln (NO) flux as a function of inverse temperature (K^{-1}) for different values of water-filled pore space (WFPS) and N addition. Also shown is the coefficient of determination (r^2) of the regression and the results of a 2-way ANOVA that assessed differences in the Arrhenius coefficients as a function of nitrogen addition and soil moisture.

	Nitrogen addition								
	0 g N/m^2			2 g N/m^2			5 g N/m^2		
Soil moisture (%WFPS)	b (ng m^{-2} s^{-1})	E_a (kJ/mol)	r^2	b (ng m^{-2} s^{-1})	E_a (kJ/mol)	r^2	b (ng m^{-2} s^{-1})	E_a (kJ/mol)	r^2
10.5	29.7 ± 9.6	70.7 ± 12	0.77	39.9 ± 6.5	95.5 ± 8	0.93	47.3 ± 10.1	113.6 ± 15	0.88
25.0	20.6 ± 7.9	42.5 ± 11	0.66	28.1 ± 5.0	59.9 ± 6	0.90	28.6 ± 6.4	60.1 ± 3	0.84
57.3	31.0 ± 8.4	71.3 ± 8	0.81	25.6 ± 7.6	57.4 ± 6	0.78	26.3 ± 7.1	58.1 ± 7	0.80
72.7	28.6 ± 6.8	66.2 ± 8	0.85	32.1 ± 7.6	73.7 ± 11	0.85	30.4 ± 8.3	68.8 ± 8	0.81

Source	DF	Intercept (b)				Activation energy (E_a)			
		SS	MS	F-ratio	p-value	SS	MS	F-ratio	p-value
Nitrogen addition (N)	2	360	180	2.6	0.09	1768	884	2.2	0.13
Soil moisture (W)	3	1545	515	7.4	<0.001	12,893	4298	10.4	<0.001
N × W	6	724	121	1.7	0.13	4539	757	1.8	0.11
Error	48	3342	70			19,766	412		
Total	60	5970				38,966			

in soil extractable NO_3^-, as nitrification rates may require several days to respond to NH_4^+ enrichment (Chen and Stark, 2000; Venterea and Rolston, 2000). Correlations between NO flux and extractable NO_3^- can be variable, and perhaps the most important first-order regulation of NO emission is excess N availability relative to C availability, which causes more N to flow through the nitrification and denitrification pipes (Davidson, 1991). Thus, our data suggest that soil N enrichment from anthropogenic N input will "increase in the size of the pipe" and cause an increase in NO efflux (Fenn et al., 1996; Li et al., 2006; Homyak and Sickman, 2014).

NO efflux is also influenced by the ecosystem N transformations (the holes) such as nitrification and denitrification. Nitrification is a two-step process involving the oxidation of NH_4^+ to nitrite (NO_2^-), an intermediary, and the further oxidation of NO_2^- to NO_3^-, while denitrification is the reduction of NO_3^- to N_2, with NO_2^-, NO, and nitrous oxide (N_2O) as intermediate products (Firestone and Davidson, 1989). Both of these biological transformations result in the production of NO. In turn, protonation of NO_2^- can produce nitrous acid (HNO_2), and chemical degradation of HNO_2 can account for an additional abiotic source of NO (Remde and Conrad, 1990; Davidson, 1992; Venterea and Rolston, 2000; Venterea et al., 2005). Excess NH_4^+ can accelerate both the biotic and abiotic production of NO by enriching NO_3^-, NO_2^-, and H^+ pools through the oxidation of NH_4^+ (Davidson, 1991).

4.2. Interactions between added N, soil moisture, and temperature

In general, the highest NO efflux was observed from soil samples treated with 5 g N/m^2 $(NH_4)_2SO_4$, 25% WFPS, and 35 °C, which is comparable to results reported for other natural (Schindlbacher et al., 2004) and managed (Laville et al., 2009) ecosystems. These environmental conditions are also typical of the early-summer and late-fall in urban chaparral ecosystems exposed to high levels of anthropogenic N deposition (Vourlitis et al., 2007a, 2009; Fenn et al., 2003b; Meixner and Fenn, 2004; Li et al., 2006).

Soil temperature is an important control on microbial activity (Lloyd and Taylor, 1994; Fang and Moncrieff, 2001), and the temperature response of NO flux was well described by the Arrhenius function, which has been observed in a variety of soils (Williams et al., 1987; Schindlbacher et al., 2004; Yu et al., 2010). Maximum rates of NO flux were observed at a soil temperature of ~35 °C, and there was a statistically significant interaction between the Arrhenius coefficients and soil water content indicating that the temperature response of NO flux varied as a function of soil water content. For example, activation energy (E_a) values varied between 42.4 and 113.6 kJ mol^{-1}, and were lowest in the 25% WFPS treatment (Table 2), indicating less kinetic energy was required to drive NO flux at this soil water content (del Prado et al., 2006). These E_a values are similar to those reported for other Mediterranean soils (Williams et al., 1987; Schindlbacher et al. 2004).

However, patterns of NO efflux in the various N, temperature and soil water treatment combinations were complex, indicating that microbial responses to temperature and/or water content depend on soil resource availability (Billings and Ballantyne, 2013). For example, rates of NO efflux in the room (25 °C) and hot water bath (35 °C) treatments peaked at 25% WFPS, but the magnitude of this peak varied as a function of N availability (Fig. 3). Considering only these treatment combinations, an increase in N availability from 0 to 2 g N/m^2 resulted in a small (9.1 ngN m^{-2} s^{-1}) increase in NO flux at 25 °C but a >2-fold increase in NO flux at 35 °C, while an increase in N availability from 2 to 5 g N/m^2 resulted in a >2-fold increase in NO flux at 25 °C but a small (9.6 ngN m^{-2} s^{-1}) increase in NO flux at 35 °C. The reason for these complex dynamics is unclear, but higher temperatures might decrease microbial N transformations because of high rates of respiration, especially in N-rich environments (Manzoni et al., 2012), and/or higher temperatures may decrease the thermal bridging of water between soil particles, which decreases water availability to nitrifying bacteria (Sakaguchi et al., 2007). Thus, the actual volume of water that was available to nitrifying bacteria may have been lower in the 35 °C/25% WFPS treatment combination, which may have limited the microbial response to an increase in available N.

Water content is the environmental factor that determines whether nitrification or denitrification will predominate in a particular soil (Davidson, 1992), and we hypothesized that NO would present an optimum response as a function of soil moisture. This hypothesis was supported from the data collected here, and these results are consistent with previous studies that have suggested that both sub- and super-optimal soil moisture levels inhibited NO efflux (Linn and Doran, 1984; Davidson, 1991; Parsons et al., 1996; Schindlbacher et al., 2004). At low soil moisture levels (≤10% WFPS) soil microbial activity may be limited by soil moisture, while at higher soil moistures, a decline in NO production may occur because of a reduction in O_2 diffusion rates and reduced diffusivity of NO, leading to the production of N_2O, and ultimately N_2 in the wettest soils (Davidson, 1991; Skiba et al., 1993). However,

in other chaparral soils Homyak and Sickman (2014) found that the highest rates of ambient NO efflux occurred in soils with <10% WFPS, which typically occurred during the warm summer when rates of plant N uptake were low but rates of N mineralization and nitrification were still high enough to support NO production and efflux. Furthermore, large episodic pulses of NO have been observed upon soil re-wetting, especially in response to fall rainfall events that mobilize labile N and C that accumulates during the dry season (Davidson, 1991; Smart et al., 1999; Homyak and Sickman, 2014). It is likely that a similar phenomenon occurred during our laboratory experiment, as mean instantaneous fluxes in excess of 120 ngN m^{-2} s^{-1} were observed in the intermediate-high N and 25% WFPS treatments after dry soils were experimentally rehydrated, which are similar in magnitude to field NO fluxes measured in response to simulated rainfall pulses.

5. Conclusions

We found that NO flux from chaparral soil was significantly altered by variations in soil temperature, moisture, and available N; however, patterns were complex, resulting in significant 2- and 3-way interactions between NO flux and the soil environmental variables. Clearly, increases in N availability lead to large increases in NO efflux, and maximum rates of NO efflux were observed at low-intermediate soil moistures (25% WFPS), which are indicative of early-summer and late-fall soil moisture conditions in southern California chaparral. NO efflux increased exponentially as a function of temperature up to 35 °C, suggesting that summer rates of NO efflux could also be high, especially after episodic rainfall events which could mobilize available N and cause a flush of NO from both biotic and abiotic processes. Our results indicate that semiarid urban shrublands in southern California can be appreciable sources of NO. Given the positive relationship between NO flux and N input, chronic, high levels of anthropogenic N deposition will enhance NO efflux from these semi-arid shrublands.

Acknowledgments

This research was supported in part by the NSF-CAREER (DEB-0133259), NIH-NIGMS-SCORE (S06 GM 59833), and the USDA-NIFA-HSI (2010-38422-21241) programs. Permission to conduct field sampling on university property was graciously granted from California State University San Marcos. The authors thank Sam Fernandez, an undergraduate student assistant, for his help in soil collection, and we are especially grateful for Thermo Electron Corporation lending us a chemiluminescence analyzer to use for the duration of the study. We acknowledge support from California State University San Marcos for the use of their graduate laboratory.

References

Aber, J.D., Nadelhoffer, K.J., Steudler, P., Melillo, J.M., 1989. Nitrogen saturation in northern forest ecosystems: excess nitrogen from fossil fuel combustion may stress the biosphere. BioScience 39, 378–386.

Andersen, I.C., Poth, M.A., 1989. Semiannual losses of nitrogen as NO and N_2O from unburned and burned chaparral. Glob. Biogeochem. Cycles 3, 121–135.

Billings, S.A., Ballantyne IV, F., 2013. How interactions between microbial resource demands, soil organic matter stoichiometry, and substrate reactivity determine the direction and magnitude of soil respiratory responses to warming. Glob. Change Biol. 19, 90–102.

Bowman, R.H., Bishop, R.E., Griffin, R.W., Jones, M.L., 1973. Soil Survey of San Diego Area, California. United States Department of Agriculture, Soil Conservation Service, United States Department of Interior, p. 127.

Bytnerowicz, A., Fenn, M.E., 1996. Nitrogen deposition in California soils: a review. Environ. Pollut. 92, 127–146.

Chen, J., Stark, J.M., 2000. Plant species effects and carbon and nitrogen cycling in a sagebrush-crested wheatgrass soil. Soil Biol. Biochem. 32, 47–57.

Cho, K.D., Peirce, J.J., 2005. Nitric oxide emissions from the soil to lower levels of the troposphere. Environ. Eng. Sci. 22, 46–57.

Davidson, E.A., 1991. Fluxes of nitrous oxide and nitric oxide from terrestri-al ecosystems. In: Rogers, J.E., Whitman, W.B. (Eds.), Microbial Production and Consumption of Greenhouse Gases: Methane, Nitrogen Oxides and Halomethanes. American Society for Microbiology, Washington (DC), pp. 219–235.

Davidson, E.A., 1992. Sources of nitric oxide and nitrous oxide following wetting and dry soil. Soil Sci. Soc. Am. J. 56, 95–102.

del Prado, A., Merino, P., Estavillo, J.M., Pinto, M., González-Murua, C., 2006. N_2O and NO emissions from different N sources and under a range of soil water contents. Nutr. Cycl. Agroecosyst. 74, 229–243. http://dx.doi.org/10.1007/s10705-006-9001-6.

Fang, C., Moncrieff, J.B., 2001. The dependence of soil CO_2 efflux on temperature. Soil Biol. Biochem. 33, 155–165.

Fenn, M.E., Poth, M.A., Johnson, D.W., 1996. Evidence for nitrogen saturation in the San Bernardino Mountains in southern California. For. Ecol. Manag. 82, 211–230.

Fenn, M.E., Haeuber, R., Tonnesen, G.S., Baron, J.S., Grossman-Clarke, S., Hope, D., Jaffe, D.A., Copeland, S., Geiser, L., Rueth, H.N., Sickman, J.O., 2003a. Nitrogen emissions, deposition, and monitoring in the western United States. BioScience 53, 391–403.

Fenn, M.E., Baron, J.S., Allen, E.B., Rueth, H.M., Nydick, K.R., Geiser, L., Bowman, W.D., Sickman, J.O., Meixner, T., Johnson, D.W., Neitlich, P., 2003b. Ecological effects of nitrogen deposition in the western United States. BioScience 53, 404–420.

Fenn, M.E., Poth, M.A., 2004. Monitoring nitrogen deposition in throughfall using ion exchange resin columns: a field test in the San Bernardino Mountains. J. Environ. Qual. 33, 2007–2014.

Fenn, M.E., Jovan, S., Yuan, F., 2008. Empirical and simulated critical loads for nitrogen deposition in California mixed conifer forests. Environ. Pollut. 155, 492–511.

Firestone, M.K., Davidson, E.A., 1989. Microbial basis of NO and N_2O production and consumption in soil. In: Andreae, M.O., Schimel, D.S. (Eds.), Exchange of Trace Gases between Terrestrial Ecosystems and the Atmosphere. John Wiley & Sons, New York, pp. 7–21.

Galloway, J.N., Dentener, C.J., Capone, D.G., Boyer, E.W., Howarth, R.W., Seitzinger, S.P., Asner, G.P., Cleveland, C.C., Green, P.A., Holland, E.A., Karl, D.M., Michaels, A.F., Porter, J.H., Townsend, A.R., Vörösmarty, C.J., 2004. Nitrogen cycles: past, present, and future. Biogeochemistry 70, 153–226.

Hintz, J., 2004. NCSS and PASS. Number Cruncher Statistical Systems. Kaysville, Utah. www.NCSS.com.

Homyak, P.M., Sickman, J.O., 2014. Influence of soil moisture on the seasonality of nitric oxide emissions from chaparral soils, Sierra Nevada, California, USA. J. Arid Environ. 103, 46–52.

Homyak, P.M., Sickman, J.O., Miller, A.E., Melack, J.M., Meixner, T., Schimel, J.P., 2014. Assessing nitrogen-saturation in a seasonally dry chaparral watershed: limitations of traditional indicators of N-saturation. Ecosystems. http://dx.doi.org/10.1007/s10021-014-9792-2.

Johnson-Maynard, J.L., Shouse, P.J., Graham, R.C., Castiglione, P., Quideau, S.A., 2004. Microclimate and pedogenic implications in a 50-year-old chaparral and pine biosequence. Soil Sci. Soc. Am. J. 68, 876–884.

Laville, P., Flura, D., Gabrielle, B., Loubet, B., Fanucci, O., Rolland, M.-N., Cellier, P., 2009. Characterisation of soil emissions of nitric oxide at field and laboratory scale using high resolution method. Atmos. Environ. 43, 2648–2658.

Li, X.Y., Meixner, T., Sickman, J.O., Miller, A.E., Schimel, J.P., Melack, J.M., 2006. Decadal-scale dynamics of water, carbon and nitrogen in a California chaparral ecosystem: DAYCENT modeling results. Biogeochemistry 77, 217–245.

Linn, D.M., Doran, J.W., 1984. Effect of water-filled pore space on carbon dioxide and nitrous oxide production in tilled and non-tilled soils. Soil Sci. Soc. Am. J. 48, 1267–1272.

Lloyd, J., Taylor, J.A., 1994. On the temperature dependence of soil respiration. Funct. Ecol. 8, 315–323.

Manzoni, S., Taylor, P., Richter, A., Porporato, A., Agren, G.I., 2012. Environmental and stoichiometric controls on microbial carbon-use efficiency in soils. New. Phytol. 196, 79–91.

Meixner, T., Fenn, M., 2004. Biogeochemical budgets in a Mediterranean catchment with high rates of atmospheric N deposition: importance of scale and temporal asynchrony. Biogeochemistry 70, 331–356.

Parsons, D.A.B., Scholes, M.C., Scholes, R.J., Levine, J.S., 1996. Biogenic NO emissions from savanna soils as a function of fire regime, soil type, soil nitrogen, and water status. J. Geophys. Res. Atmos. 101, 23683–23688.

Remde, A., Conrad, R., 1990. Production of nitric oxide in *Nitrosomonas europaea* by reduction of nitrite. Arch. Microbiol. 154, 187–191.

Remde, A., Conrad, R., 1991. Role of nitrification and denitrification for NO metabolism in soil source. Biogeochemistry 12, 189–205.

Roelle, P.A., Aneja, V.P., Mathur, R., Vukovich, J., Peirce, J., 2002. Modeling nitric oxide emissions from biosolid amended soils. Atmos. Environ. 36, 5687–5696.

Sakaguchi, I., Momose, T., Kabuchi, T., 2007. Decrease in thermal conductivity with increasing temperature in nearly dry sandy soil. Eur. J. Soil Sci. 58, 92–97.

Sawyer, J.O., Keeler-Wolf, T., 1995. A Manual of California Vegetation. California Native Plant Society, Sacramento, CA, USA, p. 471.

Schindlbacher, A., Zechmeister-Boltenstern, S., Butterbach-Bahl, K., 2004. Effects of soil moisture and temperature on NO, NO_2, and N_2O emissions from European forest soils. J. Geophys. Res. 109, D17302,. http://dx.doi.org/10.1029/2004JD004590.

Sirulnik, A.G., Allen, E.B., Meixner, T., Allen, M.F., 2007. Impacts of anthropogenic N additions on nitrogen mineralization from plant litter in exotic annual grasslands. Soil Biol. Biochem. 39, 24–32.

Sjögersten, S., Wookey, P.A., 2002. Climatic and resource quality controls on soil respiration across a forest–tundra ecotone in Swedish Lapland. Soil Biol. Biochem. 34, 1633–1646.
Skiba, U., Smith, K.A., Fowler, D., 1993. Nitrification and denitrification as sources of nitric oxide and nitrous oxide in a sandy loam soil. Soil Biol. Biochem. 25, 1527–1536.
Skiba, U., Pitcairn, L., Sheppard, L., Kennedy, V., Fowler, D., 2004. The influences of atmospheric N deposition on nitrous oxide and nitric oxide fluxes and soil ammonium and nitrate concentrations. Focus 4, 37–43.
Smart, D.R., Stark, J.M., Diego, V., 1999. Resource limitations to nitric oxide emissions from a sagebrush-steppe ecosystem. Biogeochemistry 47, 63–86.
Townsend, A.R., Howarth, R.W., Bazzaz, F.A., Booth, M.S., Cleveland, C.C., Collinge, S.K., Dobson, A.P., Epstein, P.R., Holland, E.A., Keeney, D.R., Mallin, M.A., Rogers, C.A., Wayne, P., Wolfe, A.H., 2003. Human health effects of a changing global nitrogen cycle source: frontiers in ecology and the environment. Front. Ecol. Environ. 1, 240–246.
Varella, R.F., Bustamante, M.M.C., Pinto, A.S., Kisselle, K.W., Santos, R.V., Burke, R.A., Zepp, R.G., Viana, L.T., 2004. Soil fluxes of CO_2, CO, NO, and N_2O from an old pasture and from native savanna in Brazil. Ecol. Appl. 14, S221–S231.
Venterea, R.T., Rolston, D.E., 2000. Mechanisms and kinetics of nitric and nitrous oxide production during nitrification in agricultural soils. Glob. Change Biol. 6, 303–316.
Venterea, R.T., Rolston, D.E., Cardon, Z.G., 2005. Effects of soil moisture, physical, and chemical characteristics on abiotic nitric oxide production. Nutr. Cycl. Agroecosyst. *72*, *27*–40.
Vitousek, P.M., Aber, J.D., Howarth, R.W., Likens, G.E., Matson, P.A., Schindler, D.W., Schlesinger, W.H., Tilman, D.G., 1997. Technical report: human alteration of the global nitrogen cycle: sources and consequences. Ecol. Appl. 7, 737–750.
Vourlitis, G.L., Fernandez, J.S., 2012. Changes in the soil, litter, and vegetation nitrogen and carbon concentrations of semiarid shrublands in response to chronic dry season nitrogen input. J. Arid Environ. 82, 115–122.
Vourlitis, G.L., Zorba, G., 2007. Nitrogen and carbon mineralization of semi-arid shrubland soil exposed to long-term atmospheric nitrogen deposition. Biol. Fertil. Soils 43, 611–615.
Vourlitis, G.L., Pasquini, S., Zorba, G., 2007a. Plant and soil N response of southern Californian semi-arid shrublands after 1 year of experimental N deposition. Ecosystems 10, 263–279.
Vourlitis, G.L., Zorba, G., Pasquini, S.C., Mustard, R., 2007b. Chronic nitrogen deposition enhances nitrogen mineralization potential of semiarid shrubland soils. Soil Sci. Soc. Am. J. 71, 836–842.
Vourlitis, G.L., Pasquini, S.C., Mustard, R., 2009. Effects of dry-season N input on the productivity and N storage of Mediterranean-type shrublands. Ecosystems 12, 473–488.
Williams, E.J., Parrish, D., Fehsenfeld, F.C., 1987. Determination of nitrogen oxide emissions from soils: results from a grassland site in Colorado, United States. J. Geophys. Res. 92 (D2), 2173–2179.
Yu, J., Meixner, F.X., Sun, W., Mamtimin, B., Wang, G., Qi, X., Xia, C., Xie, W., 2010. Nitric oxide emissions from black soil, northeastern China: a laboratory study revealing significantly lower rates than hitherto reported. Soil Biol. Biochem. 42, 1784–1792.